Semicond. Sci. Technol. **23** (2008) 015003 (6pp) doi:10.1088/0268-1242/23/1/015003

Barrier inhomogeneities in Au/CdSe thin film Schottky diodes

C J Panchal[1,3], M S Desai[1], V A Kheraj[1], K J Patel[1] and N Padha[2]

[1] Applied Physics Department, Faculty of Technology and Engineering, M S University of Baroda, Vadodara 390 001, Gujarat, India
[2] Department of Physics and Electronics, Dr Ambedkar Road, University of Jammu, Jammu 180 006, Jammu and Kashmir, India

E-mail: cjpanchol_msu@yahoo.com

Received 7 July 2007, in final form 18 October 2007
Published 6 December 2007
Online at stacks.iop.org/SST/23/015003

Abstract
Schottky diodes have been fabricated by depositing Au on n-type CdSe thin films using the thermal evaporation technique, and their properties have been investigated by current–voltage and capacitance–voltage measurements. At room temperature, the characteristics obey the pure thermionic emission theory and the barrier height has been found to be 0.63 eV. The barrier heights decrease, while ideality factors increase with decrease in temperature. Further, the activation energy plot does not provide the expected Richardson constant and barrier height values. The abnormal behavior of the barrier heights and the ideality factors with respect to temperature as well as the difference between the barrier heights measured from *I–V* and those from *C–V* or flat band have been explored on the basis of barrier height inhomogeneities.

1. Introduction

Cadmium selenide (CdSe) has been a promising semiconductor material used for thin film transistors [1], high efficiency solar cells [2] and gas sensors [3] and has generated curiosity for the current transport phenomenon in the CdSe Schottky diodes. The metal–semiconductor (MS) junctions have been studied extensively [4, 5] due to their technological importance in microelectronic devices. It is well known that interfaced states of the MS contacts have a dominant influence on the device performance, reliability and stability [6, 7]. The complete description of the charge carrier transport through a MS junction still remains a challenging problem [8–13].

Schottky diodes often exhibit temperature-dependent ideality factors, η, evaluated from the forward current–voltage characteristics for the thermionic emission (TE) theory. If η increases when the temperature is decreased, the phenomenon is called the T_o-effect [14–17]. The temperature dependence of the barrier height (BH), φ_{bo}, obtained from the current–voltage (*I–V*) and capacitance–voltage (*C–V*) characteristics for these diodes, has a trend opposite to that of η, namely φ_{bo} increases while the ideality factor decreases with an increase in temperature [15–19]. Therefore, there should be some error in the evaluation of the *I–V* and *C–V* characteristics of these diodes using the usual TE theory. It was shown for the T_o-effect that the error may be connected either with the lateral inhomogeneity of the barrier height, which is not taken into account in the evaluation [20, 21], or with the role of recombination and tunneling current components [22], or with an anomalous high level of thermionic field emission dominating the current [23].

In the present work, we report the fabrication of Au/*n*-CdSe Schottky diodes and determine their barrier height, φ_{bo}, and the diode ideality factor, η, from the temperature dependence of *I–V* and *C–V* characteristics. We also explore the barrier inhomogeneities by studying the variation of the barrier height and the ideality factor with respect to the temperature.

2. Experimental procedure

The CdSe thin film of thickness about 500 nm was deposited, by the thermal evaporation technique, on the pre-deposited chromium (Cr) thin film, which was deposited on the ultrasonically cleaned glass substrate. The substrate temperature for the CdSe film was kept constant at about 373 K. The vacuum of the order of 2.66×10^{-5} Pa was maintained during the evaporation. The deposition rate of

[3] Author to whom any correspondence should be addressed.

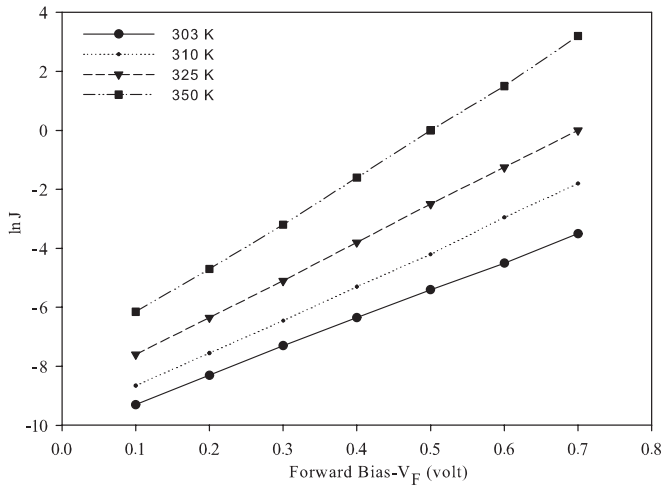

Figure 1. The current density (J_F) versus the applied forward-bias voltage (V_F) for the Au/CdSe Schottky diode at different temperatures. The linear fittings of curves have been shown by solid and dotted lines.

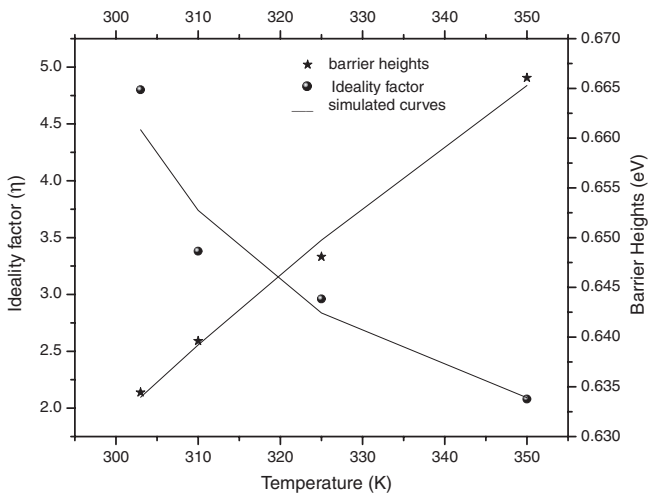

Figure 2. The ideality factor versus temperature and the zero-bias barrier height versus temperature; the solid curves are obtained by simulating the data as discussed in section 3.1.4.

the CdSe film was kept constant at about 0.5–0.8 nm s^{-1}. The CdSe thin film was then annealed at 573 K in high vacuum for two hours in order to ensure crystallization of the film as well as stable electrical measurements of Schottky diodes. For the fabrication of the Schottky diode (non-ohmic contact), a thin gold electrode film of thickness about 25 nm was deposited onto the CdSe film. The area of the Schottky diode is 2.5 × 10^{-3} cm^2. It has been observed from the preliminary study of MS contact that the Cr film shows good ohmic contacts to the CdSe film and can work as a back-metal electrode, while the gold film shows a good non-ohmic contact to the CdSe film.

The thickness and the deposition rate of the films were measured by a quartz crystal digital thickness monitor. The current–voltage measurements were carried out using a high impedance digital electrometer (Keithley 614) and a dc-voltage source. The capacitance–voltage measurements were carried out with a digital LCR bridge (Vasavi-VLCR.17D) and a dc-voltage source. The temperature-dependent *I–V* and *C–V* characteristics were observed from 303 K to 350 K.

3. Results and discussion

3.1. Forward current–voltage (I–V) characteristics

The forward current–voltage (*I–V*) characteristics of the Au/n-CdSe Schottky diodes at temperatures from 303 K to 350 K are shown in figure 1.

At first, we analyze the experimental data by the well-known thermionic emission (TE) equation at a forward bias [14]:

$$I = I_s\left[\exp\left(\frac{q(V - IR_S)}{\eta kT}\right) - 1\right] \tag{1a}$$

and for forward bias, $V \geqslant 3kT/q$,

$$I \approx I_s \exp\left(\frac{q(V - IR_S)}{\eta kT}\right), \tag{1b}$$

where I_s, the saturation current, and J_s, the saturation current density, are defined as

$$J_s = \frac{I_s}{a} = A^{**}T^2 \exp\left(-\frac{q\varphi_{bo}}{kT}\right). \tag{2}$$

The quantities a, A^{**}, T, k, q, φ_{bo} and R_S are, respectively, the diode area, the effective Richardson constant, the temperature in kelvin, Boltzmann's constant, the electronic charge, the zero bias or the apparent barrier height and the diode series resistance. The ideality factor, η, is introduced to describe the deviation of the experimental *I–V* data from the ideal thermionic emission diffusion (TED) model using the definition

$$\eta = \frac{q}{kT}\frac{dV}{d\ln J}. \tag{3}$$

The slope and intercept (on the x-axis) of the linear fit of the data using equation (1*a*) provide the values of the ideality factor (η) and saturated current density (J_S), respectively. The value of J_S so obtained on substitution into equation (2), assuming the effective Richardson constant (A^{**}) of 15.6 A cm^{-2} K^{-2} [11], provides the value of φ_{bo} at different temperatures.

3.1.1. Zero-bias barrier height and ideality factor. The zero-bias barrier height, φ_{bo}, and the ideality factor, η, derived at each temperature have been plotted in figure 2. At room temperature, the characteristics obey the thermionic emission theory; the Schottky barrier height (SBH) and the ideality factor are 0.63 eV and 4.7, respectively. Above room temperature, the barrier height and the ideality factor vary with increasing temperature. These changes are indicative of deviations from the pure thermionic emission mechanism and there is a current flow, in excess, with respect to that due to the standard thermionic emission theory.

3.1.2. Flat-band barrier height. The barrier height, φ_{bo}, as obtained from equation (2), decreases with decreasing temperature.

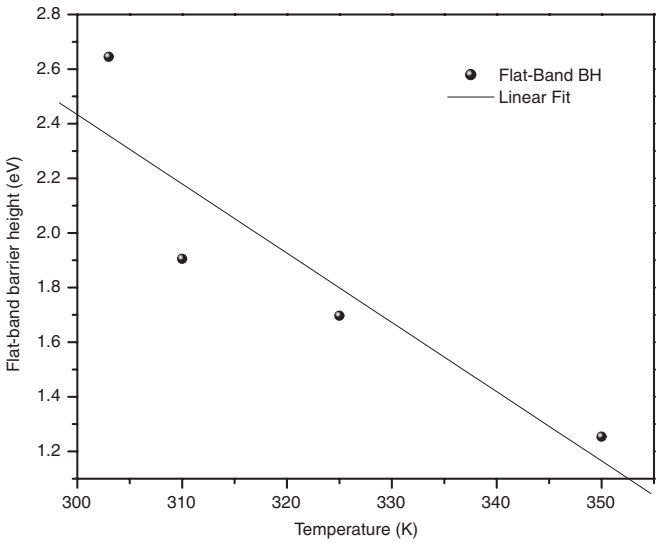

Figure 3. The flat-band barrier height, φ_b^f, versus temperature. The linear fit gives a negative temperature coefficient, $d\varphi_b^f/dT$, equal to $-(2.5 \pm 8) \times 10^{-2}$ eV K^{-1}.

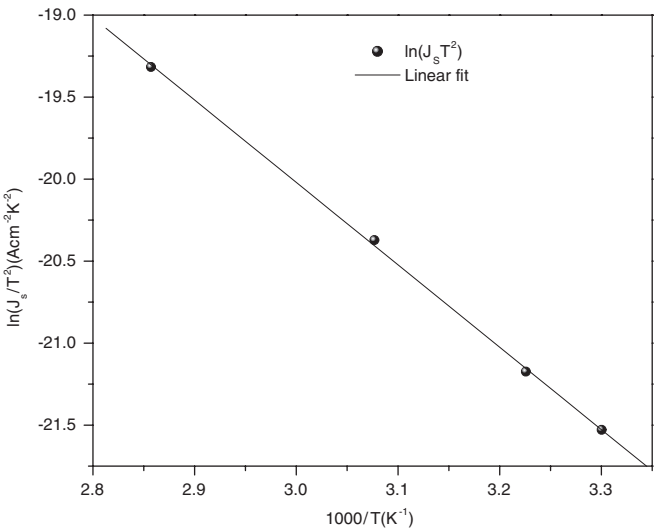

Figure 4. The plot of $\ln(J_s/T^2)$ versus $1000/T$ yields an activation energy value of 0.43 eV and an effective Richardson constant value of 2.83×10^{-3} A cm^{-2} K^{-2}. These values are lower than the corresponding reported values of the activation energy and effective Richardson constants.

Unlike this, the barrier height obtained under the flat-band conditions (in which the electric field in the semiconductor is zero) is called the flat-band barrier height, φ_b^f, and is defined as [19]

$$\varphi_b^f = \eta\varphi_{bo} - [\eta - 1]kT \ln\left[\frac{N_c}{N_d}\right], \tag{4}$$

where N_c is the effective density of states in the conduction band and N_d is the concentration of the donor in the semiconductor.

The variation of φ_b^f as a function of temperature is shown in figure 3. It is observed that φ_b^f is always larger than φ_{bo}. Furthermore, φ_b^f is found to increase with a decrease in temperature, i.e. it has a negative temperature coefficient, in a manner as reported by Werner and Guttler [16], with an average value of 1.87 eV.

A linear fit of the data in the temperature range 310–350 K gives the temperature-coefficient value of φ_b^f as $-\frac{d\varphi_b^f}{dT} = -(1.6 \pm 1) \times 10^{-2}$ eV K^{-1}. This value is close to the band-gap variation of the CdSe semiconductor with temperature.

3.1.3. Richardson plots. Figure 4 shows the usual activation energy plot, $\ln(J_s/T^2)$ versus $1000/T$, of the forward bias I–V data. The experimental data thus plotted yield a straight line with a slope giving BH at 0 K, $\varphi_{bo}(T = 0)$. The zero-bias barrier height, φ_{bo}, and the Richardson constant, A^{**}, thus obtained are 0.43 eV and 2.83×10^{-3} A cm^{-2} K^{-2}, respectively; the latter value is three orders of magnitude lower than the reported value of 15.6 A cm^{-2} K^{-2} [11], whereas the former is about 0.2 eV less than that obtained in figure 2. The variations between the obtained and the reported values may be due to the temperature dependence of the barrier height BH and ideality factor due to the existence of surface inhomogeneities in the CdSe semiconductor layer [24, 25].

3.1.4. Effect of barrier inhomogeneities. The above discrepancies of Schottky barrier parameters, namely ideality factor, η, barrier height, φ_{bo}, and Richardson constant, A^{**}, have been explored on the basis of the existence of barrier inhomogeneities resulting due to the variation in thickness and composition of an interfaced layer, non-uniformity of interfacial charges, etc [16].

Werner and Güttler [16] proposed that the above abnormal behavior can be explained by assuming a Gaussian distribution of Schottky barrier heights with a mean barrier height, φ_{bmean}, and a standard deviation, σ_s. Their relation [16] in a simpler form, proposed by Chand and Kumar [18], is given by

$$\varphi_{bo} = \varphi_{bmean} - \left(\sigma_s^2/2kT\right), \tag{5}$$

where φ_{bo} is the zero-bias barrier height or the apparent barrier height. σ_s and φ_{bmean} have been obtained, respectively, from the slope and the intercept of the straight-line portion of the φ_{bo} versus $1/T$ plot of equation (5), namely $\varphi_{bmean} = 0.867$ eV and $\sigma_s = 0.11$. φ_{bo} is then recalculated by substituting the above calculated values of φ_{bmean} and σ_s in equation (5) and is replotted along with the experimentally observed φ_{bo} versus T plot in figure 2.

The abnormal behavior of the ideality factors with temperature has also been explained by Werner and Güttler [16] by considering the potential fluctuation model using the log normal distribution function for ideality factors. Their relation [16] in a simpler form, proposed by Chand and Kumar [18], is given by

$$\frac{1}{\eta} = 1 - \gamma + \frac{q\zeta\sigma_s}{kT}, \tag{6}$$

where γ and ζ are the voltage coefficients of the mean barrier height and standard deviation respectively. Using the experimental η values, a plot of $1/\eta$ versus $1/T$ is shown in figure 5; the intercept and the slope of the linear part of the plot

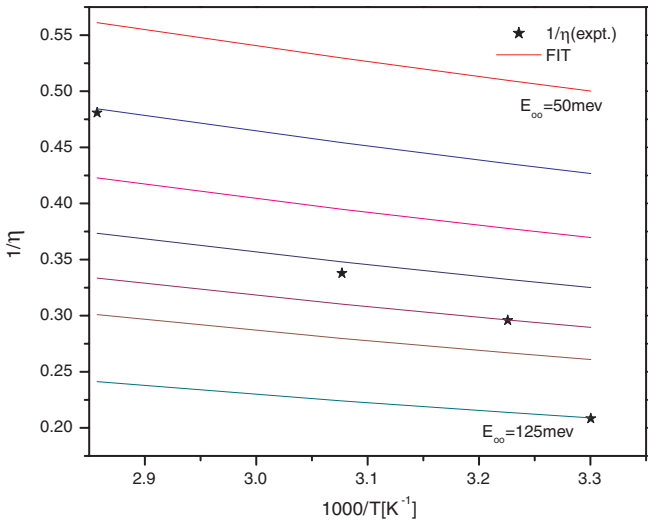

Figure 5. The reciprocal of the ideality factor versus $1/T$ gives the voltage coefficients γ and ζ.

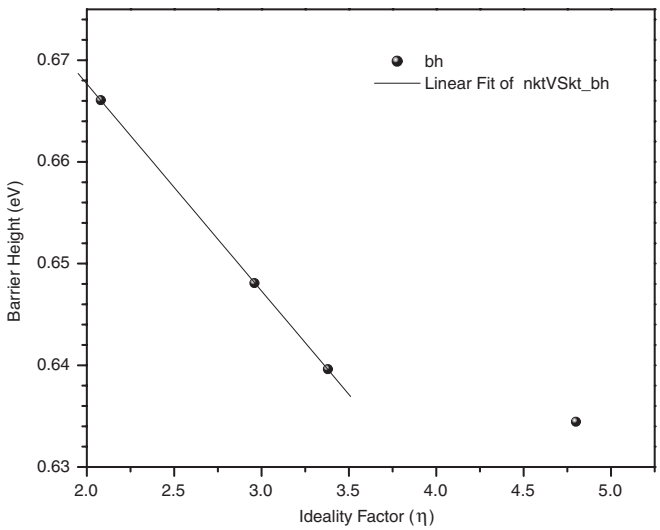

Figure 6. The above plot shows the correlation between the barrier height and the ideality factor as discussed in section 3.1.4.

gives γ and ζ, respectively. The values of γ and ζ so calculated are resubstituted in equation (6) to calculate the simulated η values at varying temperatures. The continuous curve of figure 2 represents the simulated values of η taking $\gamma = -1.112$ and $\zeta = -0.448$. On comparing the experimental and the simulated data, as per the above proposed distribution function, it is observed that the variations in the observed temperature range are well justified on the basis of barrier inhomogeneities using the Gaussian distribution of barrier heights and log normal function of ideality factors.

Sullivan *et al* [24] and Tung [25] proposed an alternative approach to the lateral inhomogeneities that are found in the Schottky barrier interfaces, i.e. the Schottky barrier consisted of laterally inhomogeneous patches of different barrier heights. The patch with lower barrier height yields a larger ideality factor and vice versa. Schmitsdroff *et al* [26] found a linear correlation between the zero-bias barrier height and the ideality factors using Tung's [25] theoretical approach. An analysis to this effect using present data has been presented in figure 6, wherein it has been observed that the barrier heights correlated linearly with the ideality factors measured in the temperatures 303 K to 325 K and justify the lateral inhomogeneities in the Schottky barrier area. Further, the extrapolation of the linear fit in the φ_{bo} versus η plot, figure 6, yields the homogeneous barrier height value of 0.708 eV at an ideality factor value of 1.01.

From the above-referred results represented in figures 2 and 4, it is observed that the deviations in the ideality factors and BHs may be due to spatially inhomogeneous BHs and potential fluctuations at the interface that consist of the low and high barrier heights [15, 16, 18, 24, 25, 27], i.e. the current through the diode will flow preferentially through the lower barriers in the potential distribution. As explained in [7, 25], the current transport across the MS interface is a temperature-activated process; at low temperatures, the current transport will be dominated by the current flowing through the patches of lower SBH and a larger ideality factor. As the temperature increases, the dominant BH will increase with temperature and bias voltage [7, 25]. The commonly observed deviations from the classical thermionic theory have been explained by the above-referred models.

Moreover, the difference between the BHs measured from *I–V* and those from *C–V* or flat-band analysis in the metal/semiconductor is also evidence for the Schottky BH inhomogeneity. The reason for this discrepancy between the measured SBHs is clear. The current in the *I–V* measurement is dominated by the current which flows through the region of low SBH, and the measured *I–V* BH is significantly lower than the weighted arithmetic average of the SBHs; on the other hand, the barrier height measured from the *C–V* or flat band is influenced by the distribution of charge at the depletion region boundary and this charge distribution follows the weighted arithmetic average of the SBHs. Therefore, the SBH determined from the zero-bias intercept assuming thermionic emission as a current transport mechanism is well below the *C–V* or flat-band-measured BH and the weighted arithmetic average of SBHs [16, 24, 28].

3.1.5. Thermionic field emission. The ideality factor is further analyzed by considering the variation in the ideality factor caused by tunneling current responsible for the thermionic field emission phenomenon. The relation of the variation in the ideality factor to temperature using this model is given by the relation [26, 29]

$$\frac{1}{\eta} = \frac{KT}{q}\left(\frac{E_o}{1-\beta}\right), \tag{7}$$

where

$$E_o = E_{oo}\coth\left[\frac{qE_{oo}}{KT}\right], \tag{8}$$

where E_{oo} is the characteristics energy and β indicates the bias dependence of the barrier height. Such a plot is shown in figure 5. The experimental ideality factors when superimposed on the theoretical curves generated using equations (7) and (8) provide E_{oo} values in the range 50–125 meV. The values of

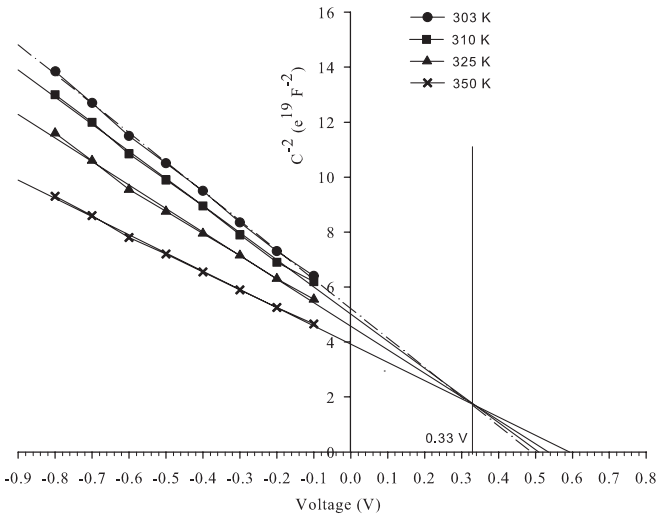

Figure 7. The *C–V* characteristics at different temperatures. The *X*-intercepts give the values for the built-in potential, V_d. The point of intersection represents the value of the built-in voltage.

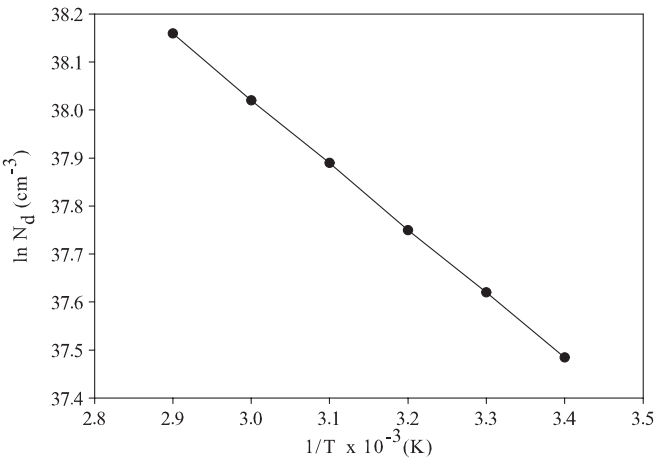

Figure 8. The logarithmic variation of the donor density with respect to the inverse of temperature.

E_{oo} so obtained does not vary as per the theoretical curves obtained using the thermionic field emission mechanism. The existence of thermionic field emission phenomena in the current transport is thus ruled out.

3.2. Capacitance–voltage characteristics

In order to access the doping concentration and barrier height, C^2 versus V_R plots (figure 7) were obtained from the *C–V* data. The *C–V* relationship is applicable to intimate MS Schottky barriers on uniformly doped materials and can be written as [4]

$$\frac{1}{C^2} = \frac{2(V_R + V_o)}{q\varepsilon_s N_D a^2}, \tag{9}$$

where V_R is the reverse bias voltage, V_o is the built-in potential or diffusion potential, which is usually measured by extrapolating the C^{-2}–*V* plot to the *V*-axis. The zero-bias barrier height from the *C–V* measurement is defined by

$$\varphi_{bo} = V_d + V_n, \tag{10}$$

where V_d is the voltage axis intercept of the above plot, $V_n = \left(\frac{kT}{q}\right) \ln\left(\frac{N_c}{N_d}\right)$ is the energy difference between the Fermi level and the bottom of the conduction band edge in CdSe and $N_c = 2\left(2\pi m_e \frac{kT}{h^2}\right)^{3/2}$ is the effective density of states in the conduction band of CdSe, where m_e = the effective mass of CdSe = 0.13 eV [32], $N_d = \frac{2}{q} K_s \varepsilon_o a^2 \left(\frac{dV}{dC^{-2}}\right)$ is the donor density of CdSe, $K_s = 10.2$ is the dielectric constant of CdSe, ε_o is the permittivity of the free space, $= 8.85 \times 10^{-14}$ F cm^{-1}, a is the area of the Schottky diode, $= 2.5 \times 10^{-3}$ cm^2.

The Schottky barrier height deduced from the *I–V* analysis includes both the image force lowering and dipole lowering effects and is also reduced by the tunneling and leakage currents. However, the capacitance–voltage measurements can be used to directly measure the barrier height. Nevertheless, it has to be noted that the measured capacitance may be considerably influenced by carrier trapping if the lifetime of the trapping levels in the semiconductor is of the same order as the period of the ac signal applied during the capacitance measurement.

For the MS Schottky barrier, the doping concentration N_d and the zero-bias barrier height ϕ_{bo} at various temperatures for the Au/n-CdSe Schottky diode have been calculated from the experimental C^{-2}–*V* characteristics as listed in table 1. As can be seen, the C^{-2}–*V* curve gave BH values higher than those derived from *I–V* measurements. Moreover, the difference between the measured *I–V* and *C–V* SBH in the metal/semiconductor barriers is also evident for the Schottky barrier height inhomogeneity. The discrepancy between *C–V* and *I–V* is due to the reason that the current in the *I–V* measurement is dominated by the current which flows through the region of low SBH. On the other hand, the *C–V*-measured BH is influenced by the distribution of charge at the depletion region boundary and this charge distribution follows the weighted arithmetic average of the SBH inhomogeneity. [16, 24, 28].

In section 3.1, we found that the flat-band barrier height φ_b^f decreases with temperature whereas in this section we find that φ_{bo} increases with temperature; this may be due to the surface states blocking the majority carrier electrons traveling from the semiconductor to the metal under forward-bias condition. This shielding effect is not present in the *C–V* characteristics; the majority carrier current is small and the barrier height is determined by modulating the depletion width [31, 32].

Figure 8 shows the temperature dependence of donor densities obtained from the *C–V* characteristics, see figure 7. The slope gives the value of the activation energy, which is found to be 0.229 eV in the temperature range 300 to 350 K; this large activation energy makes it improbable to depopulate the shallow levels in the material, and thus we infer the existence of the local states that contribute to the additional donors, which are responsible for forming the electron concentration in the material. The existence of the local states in the energy gap is usually found in polycrystalline films [33].

Table 1. Parameters from *C–V* characteristics.

Temperature T (K)	Diffusion potential V_b (V)	Effective density N_c (10^{18} cm^{-3})	Donor density of states N_d (10^{16} cm^{-3})	Energy difference $E_C - E_F = V_n$ (eV)	Barrier height (C–V) φ_{bo} (eV)
303	0.53	1.19	2.11	0.105	0.635
310	0.54	1.26	2.47	0.10	0.64
325	0.57	1.35	2.96	0.099	0.67
350	0.62	1.48	3.7	0.096	0.72

4. Conclusion

The Schottky barrier parameters such as ideality factors and barrier heights obtained from the pure thermionic emission theory alone show deviation with respect to change in temperature. Further, the variation between the SBHs measured from *I–V* and those from *C–V* or flat-band analysis in the metal/semiconductor has also been observed. These results suggest that the temperature dependence of the experimental data of the present Au/n-CdSe Schottky diodes is expressed on the basis of barrier inhomogeneities existing in the metal–semiconductor interface with a Gaussian distribution of barrier heights and log normal function of ideality factors.

References

[1] Panchal C J 2005 *Indian J. Phys.* **79** 1269
[2] Patel N G, Panchal C J, Patel P G, Makhija K K and Patel S S 1994 *Cryst. Res. Technol.* **29** 247
[3] Patel N G, Panchal C J and Makhija K K 1994 *Cryst. Res. Technol.* **29** 1013
[4] Rhoderick E H and Williams R H 1988 *Metal–Semiconductor Contacts* (Oxford: Clarendon) pp 20–48
[5] Brillson L J 1982 *Surf. Sci. Rep.* **2** 123
[6] True L E, Brinkman A W, Russel G J and Woods 1987 *J. Phys. Status Solidi* a **100** 681
[7] Horvath Zs J, Bosacchi A, Franchi S, Gombia E, Mosca R and Motta 1994 *J. Mater. Sci. Eng.* B **28** 429
[8] Selders J, Emeis N and Benekinget H 1985 *IEEE Trans. Electron Dev.* **ED-32** 605
[9] Chin V W L, Storey J W V and Green M A 1989 *Solid-State Electron.* **32** 475
[10] Sharma D K, Narasimhan K L, Kumar S and Arora B M 1989 *J. Appl. Phys.* **65** 1996
[11] Prakash O, Muurlidhara K N and Ravindra K 1990 *IETE Tech. Rev.* **7** 260
[12] Donoval D, de Sousa Pires J, Tove P A and Harman R 1989 *Solid-State Electron.* **32** 961
[13] Mikhelashvili V, Eisenstein G and Uzdin R 2001 *Solid-State Electron.* **45** 143
[14] Sze S M 1981 *Physics of Semiconductor Devices* 2nd edn (New York: Wiley) pp 255–62
[15] Chin V W L, Green M A and Storey J W V 1990 *Solid-State Electron.* **36** 407
[16] Werner S H and Guttler H H 1991 *J. Appl. Phys.* **69** 1522
[17] Aboelfotoh M O 1991 *Solid-State Electron.* **34** 51
[18] Chand S and Kumar J 1997 *J. Appl. Phys.* **82** 5005
[19] Wagner L F, Young R W and Sugerman A 1989 *IEEE Electron. Dev. Lett.* **EDL-4** 320
[20] Padovani F A and Summer G G 1965 *J. Appl. Phys.* **36** 3744
[21] Aboelfotoh M O 1987 *J. Appl. Phys.* **61** 2558
[22] Chin V W L, Green M A and Storey J W V 1993 *Solid-State Eelctron.* **36** 1107
[23] Aboelfotoh M O and Tu K N 1986 *Phys. Rev.* B **34** 2311
[24] Sullivan J P, Tung R T, Pinto M R and Graham W R 1991 *J. Appl. Phy.* **70** 7403
[25] Tung R T 1992 *Phys. Rev.* B **45** 13509
[26] Schmitsdroff R F, Kampen T U and Monch W 1997 *J. Vac. Sci. Technol.* B **15** 1221
[27] Dobrocka E and Osvald 1994 *J. Appl. Physi. Lett.* **65** 575
[28] Tung R T, Levi A F J, Sullivan J P and Sehrey F 1991 *Phys. Rev. Lett.* **66** 72
[29] Horvath Zs J 1993 *Solid-State Electron.* **36** 969
[30] West R C 1987 *Handbook of Chemistry and Physics* 1st student edn (Boca Raton, FL: CRC Press) p 82
[31] Rideout V L 1978 *Thin Solid Films* **48** 261
[32] Polla D L and Sood A K 1980 *J. Appl. Phys.* **51** 4908
[33] Tsuge H and Onuma Y 1977 *Japan. J. Appl. Phys* **16** 1973